

# NON-LINEAR PROGRESSIVE FAILURE ANALYSIS OF COMPOSITE AEROSPACE STRUCTURES

M.Günel<sup>1</sup> and A. Kayran<sup>2\*</sup>

<sup>1</sup>TAI, Ankara, Turkey, <sup>2</sup> Dept. of Aerospace Eng., METU, Ankara, Turkey

\* Corresponding author (akayran@metu.edu.tr)

**Keywords:** *progressive failure analysis, composite aerospace structures, non-linear deformation, material property degradation, Nastran, PCL code*

## Abstract

The article presents a study of geometrically non-linear progressive failure analysis of thin walled composite aerospace structures subjected to combined in-plane and out-of-plane loadings which are typically encountered in thin walled aerospace structures. Different ply and constituent based failure criteria and material property degradation schemes have been coded into a PCL code in Nastran, and progressive failure analyses of sample composite laminates with cut-outs are executed. Case studies are performed to study the effect of geometric nonlinearity on the first ply failure and progression of failure for laminated composite structures under combined in-plane and out-of-plane loadings.

## 1. Introduction

The use of composite materials in primary aerospace structures is rapidly increasing. Understanding the failure response of composite laminates which are the building blocks of composite aerospace sub-structures is essential in order to exploit the full strength of composite materials in aerospace structures and design fault tolerant structures. Thin walled composite aerospace sub-structures, such as skin panels of lifting surfaces or pressurized fuselage sections, are commonly exposed to combined in-plane and out-of-plane loadings. Composite laminates with local damages can sustain operating loads much better than their metallic counterparts. Therefore, progressive failure analysis of fiber reinforced thin walled composites is studied widely in the literature to determine the capability of composite structures to sustain loads [1-4].

In this article, two dimensional finite element based progressive failure analysis method is used to study

the first ply failure and progression of failure of composite laminates with cut-outs under combined in-plane and out-of-plane loading and geometrically non-linear deformations. In progressive failure analysis of structures which are exposed to especially out-of-plane loads, geometric non-linear effects become prominent when the structure is subjected to large displacement and rotation. In addition, in most of the previous studies on progressive failure analysis of composite structures, single load case is used. Progressive failure analysis of composite laminates under combined in-plane and out-of-plane loads is particularly important for thin walled aerospace structures which are usually subjected to combined in-plane and out-of-plane loads. Therefore, a major objective of the present study is also to investigate the significance of geometrically non-linear analysis on the progressive failure response of composite laminates under combined in-plane and out-of-plane loading.

For this purpose different ply and constituent based failure criteria and material property degradation schemes have been coded into a PCL [5] code in Nastran and progressive failure analyses of sample composite laminates with cut-outs are executed. Case studies are performed to study the effect of geometric nonlinearity on the first ply failure and progression of failure. Different ply and constituent based failure criteria and different material property degradation schemes, such as sudden degradation and gradual degradation of material properties, are also compared in terms of predicting the first ply failure and failure progression. This article presents some sample results. More comprehensive results will be presented in the conference.

## 2 Description of the PCL code

The Patran Command Language (PCL) is a

programming language which is an integral part of the MSC.Patran system. PCL can be used to write application or site specific commands and forms, create functions from all areas of MSC Patran including all applications, graphics, the user interface and the database, and completely integrate commercial or in-house programs. In the current study, different ply and constituent based failure criteria and material property degradation schemes have been coded into a PCL code which employs linear and non-linear solution types of MSC Nastran depending on the analysis type desired. For the pre-selected failure criterion, failure indices are calculated based on the strains or stresses at the shell element centers, at the mid plane of plies. In order to effectively allow material property degradation at the ply level, before the failure analysis is initiated, for each element in the finite element mesh distinct composite laminate properties with distinct two dimensional orthotropic materials for each ply are generated via the PCL code that is developed. Thus, stiffness reduction scheme is implemented easily for each failed ply by referencing the element property identification and material identification numbers of the failed ply. Progressive failure analysis continues until the ultimate laminate failure or until a prescribed load level is reached. Currently, linear static, large displacement-small strain non-linear static (Sol 106) and large displacement-large strain non-linear static (Sol 600) solution types of Nastran are implemented in the PCL code.

## 2.1 Progressive failure analysis method

In the present study, strains and stresses, which are calculated at the mid-plane of the plies by the desired solution type, are used in calculating the failure indices for the failure criterion selected. Currently, plane stress failure criterion of Hashin [6] and Tsai-Hill failure criterion [7] are implemented in the PCL code. In this article, results obtained by Hashin failure criterion are presented. In the conference, results obtained by the Tsai-Wu failure criterion will also be presented. Material property degradation method that is used with the mode dependent failure criteria depends on the mode of failure. For the two dimensional lamination theory with the transverse shear deformation effects included, degraded properties for the fiber and matrix failure modes are given separately by Eqs.(1) and (2) [1].

### Fiber failures:

$$(E_1, G_{12}, G_{13}, \nu_{12}) = R^*(E_1, G_{12}, G_{13}, \nu_{12}) \quad (1)$$

### Matrix failures:

$$(E_2, G_{12}, G_{23}, \nu_{21}) = R^*(E_2, G_{12}, G_{23}, \nu_{21}) \quad (2)$$

where the material property degradation factor  $R$  in Eqs.(1) and (2) can be adjusted to degrade the properties gradually or suddenly.

For the plane stress state, failure index of the Tsai-Wu ply failure criterion is calculated by [7]

$$F_1 \sigma_1 + F_{11} \sigma_1^2 + F_{12} \sigma_1 \sigma_2 + F_2 \sigma_2 + F_{22} \sigma_2^2 + F_{66} \tau_{12}^2 = FI \quad (3)$$

where

$$F_1 = \frac{1}{X_T} - \frac{1}{X_C} \quad F_{11} = \frac{1}{X_T X_C} \quad F_2 = \frac{1}{Y_T} - \frac{1}{Y_C} \quad (4)$$

$$F_{22} = \frac{1}{Y_T Y_C} \quad F_{66} = \frac{1}{S^2} \quad F_{12} = \frac{-1}{2\sqrt{X_T X_C Y_T Y_C}} \quad (5)$$

In the literature, material property degradation associated with failure predicted by the mode independent Tsai-Wu failure criterion is implemented by identifying a mode of failure, which is based on the stress component that contributes maximum to the failure index. For instance, if the maximum contribution to the failure index is due to fiber direction stress  $\sigma_1$ , then fiber failure is assumed. Similarly, if maximum contribution to failure index is due to transverse stress  $\sigma_2$  or shear stress  $\tau_{12}$ , then matrix failure is assumed. However, this method of material property degradation disregards the contribution of all stress components and puts the blame on only one stress component in order to identify a failure mode. In the present study, material property degradation method used with the Tsai-Wu failure criterion is modified, and the material property degradation factor, which is selected in the beginning of the analysis, is manipulated to yield two separate degradation factors that are to be used with the fiber and matrix failure modes, which are assumed to occur simultaneously. The decision on the separate degradation factors is based on the relative magnitudes of stress components, which are responsible for fiber and matrix failures. For this purpose, failure indices corresponding to failure modes are initially separated as:

$$FF = F_1 \sigma_1 + F_{11} \sigma_1^2 + F_{12} \sigma_1 \sigma_2 * \left( \frac{|\sigma_1|}{|\sigma_1| + |\sigma_2|} \right) \quad (6)$$

$$MF = F_2 \sigma_2 + F_{22} \sigma_2^2 + F_{66} \tau_{12}^2 + F_{12} \sigma_1 \sigma_2 \left\{ \frac{|\sigma_2|}{|\sigma_1| + |\sigma_2|} \right\} \quad (7)$$

where  $FF$  is the fiber failure index,  $MF$  is the matrix failure index. If the pre-selected degradation factor is  $R$ , then the requirement from the degradation factor ( $R_f$ ) associated with fiber failure is that  $R_f$  should be equal to 1 when the fiber failure index is 0, and  $R_f$  should be equal to  $R$  when the fiber failure index is 1. The same logic holds for degradation factor ( $R_m$ ) associated with the matrix failure. For the intermediate values of the fiber and matrix failure indices, a decay function, which is suitable for the pre-selected degradation factor  $R$ , is selected. The choice of the decay function is arbitrary and it can be tuned so that results of progressive failure analysis matches available experimental failure data. For sudden degradation, it is expected that the degradation factors associated with fiber and matrix failures should decay fast with the failure index, and for gradual degradation, gradual decay of the degradation factors with the fiber and matrix failure indices is more reasonable. In this study, for sudden degradation, degradation factor  $R$  is taken as 0.001, and the decay functions are selected as  $exp(-6.91FF)$ ,  $exp(-6.91MF)$ . Gradual degradation results will be presented in the conference.

## 2.2 Color coding used during progressive failure

Currently, in the PCL code, color coding used to visualize the failure progression does not distinguish the mode of failure and the failed ply. However, one can extract the mode of failure and ply number of the failed ply from the PCL code easily. During the color coding, depending on the number of failed plies different color is used. Thus, irrespective of the ply number of the failed ply in an element and the mode of failure, an element with one/two/three/... number of failed plies is painted with different colors. The following failure color coding is used for the sample application presented in this article.

- |   |   |   |   |
|---|---|---|---|
|  1 ply ;   |  2 plies ; |  3 plies ; |  4 plies |
|  5 plies ; |  6 plies ; |  7 plies ; |  8 plies |

## 3 Model description and laminate definition

Figure 1 shows the geometry, boundary definition and FE mesh of the 400 mm x 200 mm composite laminate with a circular cut-out of 100 mm in diameter at the center. Boundaries are denoted as W,E,N,S and C indicating West, East, North, South and cut-out boundaries, where the boundary conditions (1: x displ. ; 2: y displ. ; 3: z displ. ; 4: x-rotation; 5: y rotation) are specified, respectively. Composite laminate is composed of eight, 0.1308 mm thick T300/N5208 plies. The test laminate is balanced symmetric laminate with a stacking sequence [0/90/45/-45]<sub>s</sub>. Layer material is typical T300/5208 pre-preg material whose properties are:

$$E_1 = 132.38 \text{ GPa}, E_2 = 10.76 \text{ GPa}, \nu_{12} = 0.24$$

$$G_{12} = G_{13} = 5.66 \text{ GPa}, G_{23} = 3.38 \text{ GPa},$$

$$X_t = 1513.4 \text{ MPa}, X_c = 1696 \text{ MPa},$$

$$Y_t = 44 \text{ MPa}, Y_c = 44 \text{ MPa}, S = 86.87 \text{ MPa}$$

Progressive failure analysis of the laminate is performed for four different load cases summarized in Table 1 along with the boundary conditions used. In the load cases studied, uniformly distributed tension and compression loads are applied from the east edge E as shown in Fig.1, and uniform pressure is applied on the top surface. For the tensile loading, symmetry boundary conditions are applied along the mid-lines between the outer boundaries and inner boundary of the cut-out to simulate tensile test, as shown in Fig. 1 and indicated in Table 1. In the analyses, for the combined pressure and axial loading, pressure is allowed to follow deformation but axial load is assumed to have a fix direction.

## 4 Sample results of progressive failure analyses

### 4.1 Pure gradual tensile loading (load case 1)

Progressive failure analysis of the composite laminate under pure gradual tensile loading is performed by the linear static (Sol 101) and implicit non-linear (Sol 600) solution types of Nastran [8] using sudden material property degradation scheme. Figure 2 shows the common first ply failure location which is determined by the two solvers. First ply failure loads are determined as 1320 N by both linear and geometrically non-linear analysis, and first ply failure mode is identified as the matrix tension in the 90 plies (plies 2 and 7). In case of pure

in-plane tensile loading, geometrically non-linear analysis and linear analysis predict similar failure progression plots, as expected.

#### 4.2 Pure gradual pressure loading (load case 2)

Progressive failure analysis results for pure pressure loading are obtained for the load case 2 by using the implicit nonlinear solution type (Sol 600) of Nastran. Figure 3 shows the first ply failure plot which corresponds to a pressure of 0.15 MPa, and Figs. 4 shows the failure plots at an intermediate load step, and Fig.5 shows the ultimate failure. In case pure pressure loading, initial failure occurs near the edge of the cut-out along the W-E line. It is seen that although the laminate has same boundary conditions along the four edges, for the particular laminate stacking sequence, failure progression is not symmetric with respect to the cut-out, but rather failure progression is somewhat anti-symmetric with respect to the cut-out. Figures 4 and 5 show the somewhat anti-symmetric failure progression more clearly. Anti-symmetric appearance of failure progression is attributed to the position of the  $\pm 45^\circ$  layers within the laminate. For the particular laminate,  $-45^\circ$  layers are closer to the mid-plane of the laminate, therefore there are slight differences among the in-plane stresses in the  $45^\circ$  and  $-45^\circ$  layers. For the pre-preg material, since the transverse strength ( $Y_t$ ) is very low, matrix tension is seen to be the dominant failure mode. For instance, under the pressure loading, transverse stress, which contributes to the matrix tensile failure in the  $45^\circ$  ply (3<sup>rd</sup> ply) of the elements along the  $45^\circ$  SW-NE line is slightly higher than the transverse stress in the  $-45^\circ$  ply (4<sup>th</sup> ply) of the elements along the  $-45^\circ$  NW-SE line. Such differences in the stresses are the main cause for the anti-symmetric appearance of failure progression. Interestingly, ultimate failure does not occur along lines which cut through the hole, but rather ultimate failure is predicted to occur along the shorter side of the laminate, somewhere between the cut-out and the left and right edges of the laminate.

For the pure pressure loading, another case study is performed to compare the failure results of large deformation-small strain analysis (Sol 106) and large deformation-large strain analysis (Sol 600). Large deformation-small strain analysis predicted the same first ply failure pressure (0.15 MPa) as the large deformation-large strain analysis. Figures 6 and 7 present the failure plots which are determined

by the solution types 106 and 600 of Nastran at a pressure load of 0.55MPa, respectively. It is seen that for the particular load level, the use of small strain or large strain analysis does not have appreciable effect on the progression of failure. Slight differences are due to the differences in the in-plane stresses determined by the small and large strain analyses.

#### 4.3 Gradual tension loading under constant pressure (load case 3)

Progressive failure analysis is performed by the large deformation-large strain (Sol 600) solution type of Nastran using sudden material property degradation scheme. In the gradual tension loading under constant pressure, initially first ply failure is determined at the pure pressure loading of 0.12 MPa. Following the first ply failure, tensile force is gradually increased and failure is progressed. Figure 8 shows the failure plot when a very low tensile force of 100 N is applied together with the pressure. Figures 8-11 show the failure progression plots between the first ply failure (FPF) and ultimate failure. In this load case, as seen in Fig. 8, first ply failure occurs at the intersection of W-E axis and the edge of the cut-out in the 0 degree bottom ply (ply 1) in matrix tension mode. It should be noted that pressure loading causes axial loading in the y direction in the laminate. Although the x direction stresses at the intersection of the edge of the cut-out and the N-S direction are higher than the y direction stresses at the intersection of the edge of the cut-out and the W-E direction, matrix tension failure is found to be more critical due to low transverse strength of T300/N5208 pre-preg layer. However, after the first ply failure, as the tensile force is increased gradually, failure progresses along the N-S direction from the edge of the hole, as expected. Finally, as Fig.11 shows, ultimate failure is evident due to the failure of all plies of all elements along the N-S direction from the edge of the cut-out.

In case of gradual tension loading under constant pressure, linear analysis predicts a first ply failure pressure of 0.006 MPa which is much lower compared to the FPF pressure of 0.12 MPa predicted by the non-linear analysis. Figures 12 and 13 compare failure plots obtained by linear (Sol 101) and non-linear (Sol 600) analysis, respectively. These plots are obtained at a tensile force of 3500 N which is applied on top of first ply failure pressures

of 0.006 MPa and 0.12 MPa predicted by linear and non-linear analysis. Figures 12 and 13 clearly show that in case of out-of-plane loading, linear analysis predicts much severe failure progression, and highly overestimates the state of failure in the laminate.

**4.4 Gradual compression loading under constant pressure (load case 4)**

A case study is performed by the implicit nonlinear solution type of Nastran (Sol 600) to compare the state of failure progression between compressive and tensile loading of the laminate under a constant pressure load of 0.16 MPa. Figure 14 shows the failure plot at a tensile load of 1550N, and Figure 15 shows the failure plot at a compressive load of 1550N. Figure 15 shows that due to the secondary bending effect of the compressive load, laminate is more stressed, and failure is more spread compared to combined pressure and tensile load case.

**Conclusion**

Progressive failure analysis of a composite laminate with a central cut-out is presented. For this purpose, a PCL code is developed which has the capability of performing progressive failure analysis using linear and non-linear solution types of Nastran. First ply failure and failure progression plots are presented for different load cases using the mode dependent Hashin failure criterion. More comprehensive results, including the progressive failure analysis results of Tsai-Wu failure criterion and results of gradual material property degradation scheme, will be presented in the conference. Failure analysis results show that under combined in-plane and out-of-plane loadings, non-linear analysis predicts much lower first ply failure loads compared to linear analysis. Results also show that combined pressure and compressive loading is more critical compared to combined pressure and tensile loading due to the secondary bending effect of the compressive load.

**References**

[1] Y.S.N. Reddy, C.M.D. Moorthy and J.N. Reddy, "Non-linear progressive failure analysis of laminated composite plates", *Int. J. Non-linear Mechanics*, 30(5), pp. 629-649, 1995.  
 [2] D.W. Sleight, "Progressive failure analysis methodology of laminated composite structures", NASA/TP-1999-209107.

[3] T.E. Tay, G.Liu, V.B.C. Tan, X.S. Sun and D.C. Pham, "Progressive failure analysis of composites", *Journal of Composite Materials*, 42(18), pp. 1921-1966 (2008).  
 [4] M.R. Garnish and V.M.K. Akula, "Review of degradation models for progressive failure analysis of fiber reinforced composites", *Applied Mechanics Reviews*, 62, pp. 1-33, 2009.  
 [5] MSC. Software Corporation, PCL and Customization guide, MSC Software Corporation, 2001.  
 [6] Z. Hashin "Failure criteria for unidirectional fiber composites", *Journal of Applied Mechanics*, 47, pp. 329-334 (1980).  
 [7] S.W. Tsai, "A general theory of strength for anisotropic materials", *Journal of Composite Materials*, 5, pp. 58-80 (1971).  
 [8] MSC. Software Corp., MSC Doc. Library, 2005.

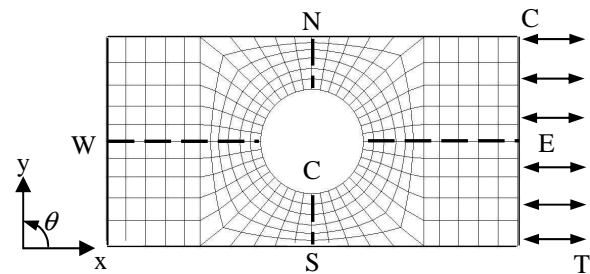


Fig. 1 Geometry and boundary definition

Table 1 Load cases and boundary conditions

| Load Cases <sup>1</sup> (LC) | Boundary conditions |
|------------------------------|---------------------|
| 1                            | T                   |
| 2                            | P                   |
| 3                            | P +T                |
| 4                            | P+C                 |

<sup>1</sup>T: Tension, C: Compression, P: Pressure

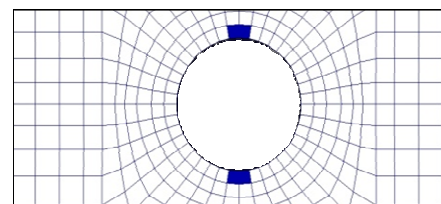


Fig 2 First ply failure; Load case:1, T=1320 N

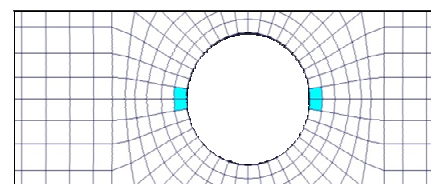


Fig. 3 First ply failure; Load case:2, P=0.15 MPa

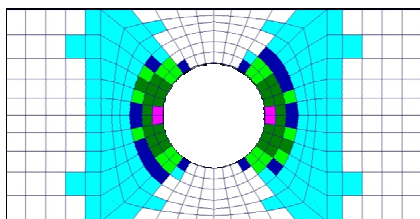


Fig. 4 Load case:2, P=0.4 MPa

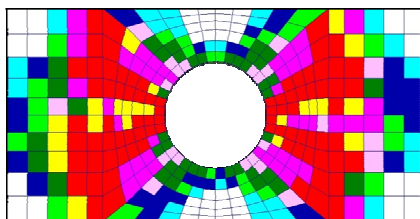


Fig. 5 Ultimate failure; Load case:2, P=0.78 MPa

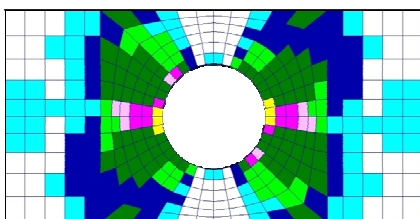


Fig. 6 Load case:2, Sol 106, P=0.55 MPa

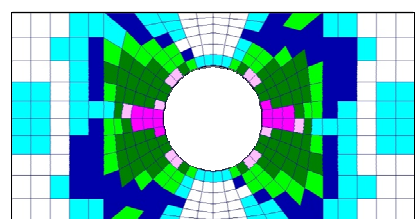


Fig. 7 Load case:2, Sol 600, P=0.55 MPa

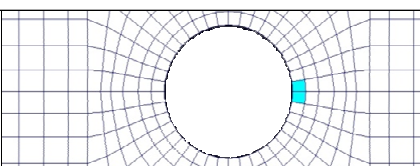


Fig. 8 First ply failure; LC:3, P=0.12 MPa T=100N

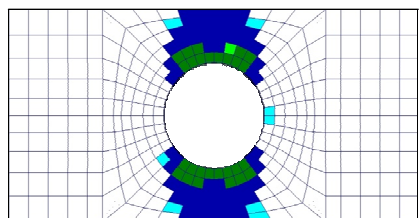


Fig. 9 Load case:3, P=0.12 MPa T=2900N

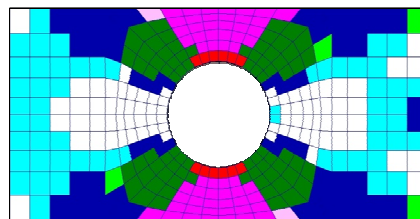


Fig. 10 Load case :3, P=0.12 MPa T=4500N

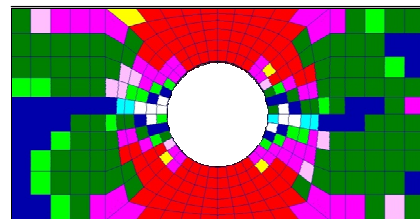


Fig. 11 Ultimate F.; LC: 3, P=0.12 MPa T=5900N

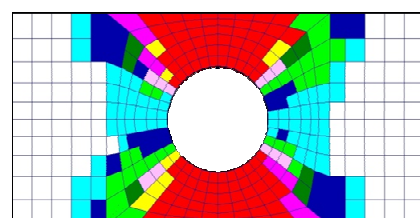


Fig. 12 Linear A., LC:3, P=0.006 MPa T=3500N

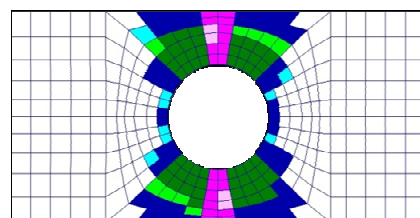


Fig. 13 Nonlinear A., LC:3, P=0.12 MPa T=3500N

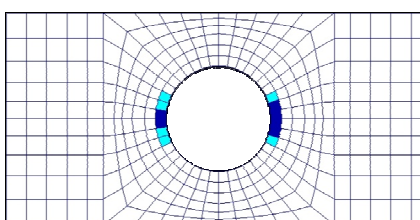


Fig. 14 Load case:3, P=0.16 MPa, T=1550N

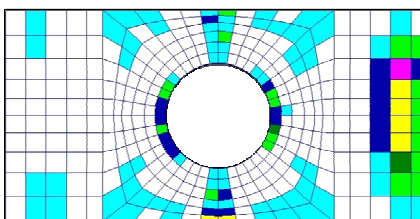


Fig. 15 Load case:3, P=0.16 MPa, C=1550N